

Quantum liquid of vortices in superconductors at $T=0$

Gianni Blatter, Boris Ivlev,* and Yuri Kagan†

Theoretische Physik, Eidgenössische Technische Hochschule–Hönggerberg, CH-8093 Zürich, Switzerland

Martijn Theunissen, Yakov Volokitin, and Peter Kes

Kamerlingh Onnes Laboratorium, Leiden University, Postbus 9506, 2300 RA Leiden, The Netherlands

(Received 19 July 1994)

We investigate the existence of a $T=0$ quantum melting transition in the vortex system of a type-II superconductor. We find that homogeneous high-resistance thin films are good candidates for the observation of this effect. We calculate both the continuous dislocation-mediated melting line $B_m^d(T)$ as well as the first-order melting line $B_m^G(T)$ driven by Gaussian fluctuations and present the resulting H - T phase diagram. At low temperatures the melting line B_m^G extrapolates to a value below the upper critical field, resulting in a quantum liquid state in the region $B_m^G < B < H_{c2}$.

One of the most fascinating phenomena in the field of quantum statistical mechanics is the occurrence of a $T=0$ phase transition driven solely by quantum fluctuations. Nature provides us with only a few such systems, the most famous example being the solid to liquid transition in He with decreasing pressure. In this paper we show that the Abrikosov vortex lattice in a type-II superconductor undergoes a $T=0$ quantum melting transition and we discuss the most favorable system conditions rendering this phenomenon accessible to experimental observation. We find that homogeneous high-resistance thin films close to the superconductor-insulator transition are good candidates for the observation of a quantum melting transition in the vortex system, with the transition to the vortex liquid phase taking place close to the upper critical field H_{c2} .

The influence of quantum fluctuations on the melting of the vortex lattice has been studied before in the high-temperature cuprate superconductors.¹ The parameter determining the importance of quantum fluctuations is the resistance ratio $Q=R_{\text{eff}}/R_Q$, where $R_Q=\hbar/e^2\approx 4.1\text{ k}\Omega$ is the quantum resistance and $R_{\text{eff}}=\rho_n/s$, ρ_n denoting the normal-state resistivity and s the relevant scale for the fluctuations. The copper oxide superconductors with their large normal-state resistivity ρ_n and short coherence length ξ (or short layer separation d) produce a large ratio $Q\approx 0.1$, rendering quantum effects important in these materials, as exemplified by the observation of quantum creep,^{2–5} a classic low-temperature quantum phenomenon. The influence of quantum fluctuations on the vortex-lattice melting transition⁶ is more difficult to resolve due to the competition with thermal fluctuations. A careful analysis shows⁷ that quantum fluctuations become appreciable at high fields and assist the thermal ones in the melting of the vortex lattice; however, an unambiguous verification of quantum melting relies on a low-temperature experiment involving extremely high magnetic fields. Furthermore, the oxides belong to the class of clean superconductors where the Hall component in the vortex dynamics⁸ and the occurrence of dispersive effects in the transport coefficients⁹ complicate the theoretical analysis.⁷

The above discussion then shows that favorable material parameters for the experimental observation of a quantum melting transition in the vortex system involve a large resistivity ρ_n , a moderate zero-temperature upper critical field H_{c2} , and a small length scale s for the fluctuations. The last requirement is in conflict with the small value required for H_{c2} , except for a thin film where the relevant scale for the fluctuations is given by the film thickness d rather than the coherence length ξ . Thin films of a conventional low- T_c material close to the superconductor-insulator transition possess a large quantum resistance ratio $Q\lesssim 1$ and thus are good candidates for the observation of this effect.

The melting of a two-dimensional (2D) crystal is an interesting phenomenon in itself: Depairing of (edge) dislocations at the Berezinskii-Kosterlitz-Thouless transition temperature¹⁰

$$T_m^d = A \frac{c_{66} a_0^2 d}{2\sqrt{3}\pi} \quad (1)$$

replaces the low-temperature quasisolid phase characterized by algebraically decaying correlations with a vortex liquid above the transition (we set the Boltzmann constant $k_B=1$). Here,

$$c_{66} = [\Phi_0 H_{c2} / (8\pi\lambda)^2] b(1-b)^2(1-0.3b)$$

is the (bulk) shear modulus, $a_0^2 = \Phi_0/B$ is the unit cell area ($\Phi_0 = hc/2e$ is the flux unit), d is the film thickness, and $b = B/H_{c2}(T)$ denotes the reduced magnetic field. The upper critical field H_{c2} and the London penetration depth λ are given by the appropriate dirty-limit expressions.^{11,12} The numerical constant $A\approx 0.65$ accounts for the renormalization of the shear modulus at the transition.^{13,14} With c_{66} depending both on temperature and field, Eq. (1) determines the shape of the dislocation-mediated melting line $B_m^d(T)$. This finite-temperature transition is a classic example for an entropy-driven transition: T_m^d is determined by the competition between the inner energy $E_d = (c_{66} a_0^2 d / \sqrt{3}\pi) \ln(L/a_0)$ (the energy to create a dislocation) and the entropy $T \ln(L^2/a_0^2)$ (L = sample size). The quantum melting of a crystal at

$T=0$ is fundamentally different from this finite-temperature melting scenario: Here the competition is between an ordered and a disordered ground state. Whereas the crystalline arrangement produces a very pronounced potential with deep minima and high maxima, the potential landscape is much smoother in a disordered (liquid) state. As a result, the bottom (top) of the potential-energy distribution is increased (lowered) in the disordered state as compared with the crystalline one (see Fig. 1). Classically, the ordered state is that of lowest energy and the crystal never melts at $T=0$. However, quantum fluctuations make the particles probe also higher-energy configurations and the ground-state energy increases (zero-point energy). This increase in energy is larger for the crystal state with its steep potential landscape. As a result, quantum fluctuations can drive the energy of the ordered state above the disordered one and the crystal melts. The physics of this melting transition is well captured by the Lindemann criterion, stating that the crystal melts as the mean displacement amplitude $\langle u^2 \rangle^{1/2}$ for the lattice constituents increases beyond a fraction $c_L < 1$ of the lattice constant a_0 ; the condition for melting then is $\langle u^2 \rangle = c_L^2 a_0^2$. The Lindemann number c_L is typically^{15,16} of the order of 0.1–0.3. In general, the mean squared displacement amplitude $\langle u^2 \rangle$ is driven by the combination of quantum and thermal fluctuations

$$\langle u^2 \rangle = \frac{\hbar}{i} \int_{-\infty}^{\infty} \frac{d\omega}{2\pi} \coth \frac{\hbar\omega}{2T} \int_0^{k_{\text{BZ}}} \frac{dk_z}{\pi} \int_0^{K_{\text{BZ}}} \frac{dK^2}{4\pi} \left[\frac{1}{c_{66}K^2 + c_{44}k_z^2 - i\omega\eta} + \frac{1}{c_{11}K^2 + c_{44}k_z^2 - i\omega\eta} \right]. \quad (2)$$

The tilt and compression moduli are both dispersive, and close to H_{c2} we can use the simplified expressions¹⁸

$$c_{44} \approx B^2(1-b)/4\pi\lambda^2k^2$$

and

$$c_{11} \approx c_{66} + B^2(1-b)^2/2\pi\lambda^2\xi^2k^4, \quad k^2 = K^2 + k_z^2 > (1-b)/\xi^2.$$

The viscous drag coefficient is given by the usual Bardeen-Stephen expression, $\eta \approx BH_{c2}/c^2\rho_n$. No dispersion effects complicating matters⁷ appear in the dirty limit considered here. The \mathbf{k} -space integration extends over the (circularized) Brillouin zone with $K_{\text{BZ}}^2 = 4\pi/a_0^2$; the appropriate cutoff k_{BZ} depends on the actual situation; see later. The frequency integration is divergent at $T=0$ and we introduce the high-frequency cutoff $\hbar\omega_{\text{max}} \approx 2\Delta \tanh(\Delta/2T)$, $\Delta \approx 1.76T_c$ [for $\omega > \omega_{\text{max}}$ the diffusion length $(e_F/ne^2\rho_n\omega)^{1/2}$ becomes less than ξ and neighboring vortices are dynamically decoupled].

Let us first focus on the 2D limit relevant for thin films with $d < \xi$. In this case the tilt modes are absent and we can substitute the k_z integral in (2) by $\int dk_z/\pi = 1/d$. An additional complication to be dealt with at finite temperatures is the $K \rightarrow 0$ logarithmic divergence in $\langle u^2 \rangle$ leading to the loss of long-range order in the Berezinskii phase.¹⁹ These long-wavelength modes are irrelevant in the Lindemann criterion which is only concerned with the short-range order in the lattice extending over a few lattice constants. We will thus cut off the $K \rightarrow 0$ diver-

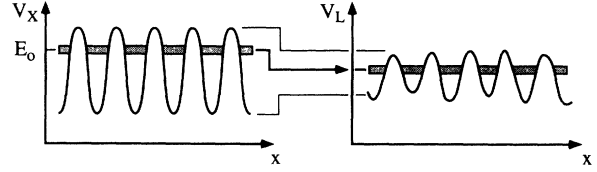


FIG. 1. Potential landscape for the crystalline (V_X) and for the disordered/liquid (V_L) arrangement of the vortex system. The bottom (top) of the potential-energy distribution is shifted up (down) in the disordered structure as compared with the ordered one. Accounting for the zero-point motion of the vortices, the steep energy landscape of the crystalline state can produce a higher ground-state energy than the smoother disordered potential and the true ground state becomes the liquid one.

and the Lindemann criterion defines a first-order melting transition within the H - T phase diagram which is driven by Gaussian fluctuations and which we denote by $B_m^G(T)$. The solid-liquid phase boundary then is given by the minimum of $B_m^d(T)$ and $B_m^G(T)$. In the following we calculate the mean squared displacement amplitude $\langle u^2 \rangle$ within a standard quantum statistical formalism both in the 2D limit (ultrathin films with $d < \xi$) and in 3D (films with $d > \xi$).

We start out with the fluctuation-dissipation theorem¹⁷ for the more general 3D case:

gence at half the Brillouin zone, which is tantamount to considering fluctuations involving next-nearest neighbors in the lattice. The result for the mean squared displacement amplitude can be split into a zero- (f_0) and a finite-temperature (f_T) contribution:

$$\frac{\langle u^2 \rangle}{\xi^2} = \frac{4}{\pi^2} \frac{R^{\square}}{R_Q} [f_0(\alpha, \beta) + f_T(\alpha, \gamma)],$$

$$f_0 = \frac{1}{4} \int_0^1 dx \left\{ \ln \left[1 + \frac{\beta^2}{x^2} \right] + \ln \left[1 + \frac{\beta^2 x^2}{(x^2 + \alpha)^2} \right] \right\}, \quad (3)$$

$$f_T = \frac{\gamma^2}{2} \int_0^{\infty} dy y (\coth y - 1) \times \int_0^1 dx \left[\frac{\Theta(x - \frac{1}{2})}{x^2 + \gamma^2 y^2} + \frac{x^2}{(x^2 + \alpha)^2 + \gamma^2 x^2 y^2} \right].$$

The parameters are $\alpha = 4/b(1-0.3b)$,

$$\beta = \eta\omega_{\text{max}}/c_{66}K_{\text{BZ}}^2 = 8/[pb(1-b)^2(1-0.3)],$$

and $\gamma = t(2\pi T_c/\epsilon_0 d)(R_Q/R^{\square}b)$; $R^{\square} = \rho_n/d$ is the sheet resistance, $t = T/T_c$ denotes the reduced temperature, and $\epsilon_0 = (\Phi_0/4\pi\lambda)^2$. The $\beta \rightarrow \infty$ ($b \rightarrow 1$) limit for f_0 is $f_0 \approx \ln(\beta/2.45)$. At low temperatures $f_T \approx 0.4\gamma^2$ whereas at high temperatures we obtain the result $f_T \approx (\pi/4)\gamma \ln(R/a_0)|_{R=2a_0}$, i.e.,

$$\langle u^2 \rangle \approx (T/4\pi c_{66}d) \ln(R/a_0)|_{R=2a_0}.$$

Combining the Lindemann criterion $\langle u^2 \rangle = c_L^2 a_0^2$ with

the expression (3) we obtain the melting line $B_m^G(T)$. The result for an optimized amorphous thin metal film [e.g., based on MoGe,²⁰ Nb₃Ge,²¹ or Bi (Ref. 22)] is shown in Fig. 2, together with the dislocation-mediated melting line $B_m^d(T)$. We have chosen a density $n=10^{23}$ cm⁻³, a resistivity $\rho_n=300$ $\mu\Omega$ cm, and a thickness $d=25$ Å, resulting in a sheet resistance $R^\square=1.2$ k Ω and a mean free path $l\approx 2$ Å. The critical temperature was chosen $T_c=2$ K leading to an upper critical field $H_{c2}=4.2$ T. The Lindemann number $c_L=0.25$ has been used.¹⁶ As expected, the dislocation-mediated melting mechanism wins over the Gaussian fluctuations at high temperatures, $B_m^d(T) < B_m^G(T)$ and hence $B_m(T)=B_m^d(T)$. On approaching zero temperature, however, the dislocation-mediated melting line approaches H_{c2} , whereas quantum fluctuations lead to a melting transition *below* the upper critical field. Using the above results we find a $T=0$ quantum melting transition at

$$B_m^G = H_{c2} \left[1 - 1.2 \exp \left[- \frac{\pi^3 c_L^2 R_Q}{4 R^\square} \right] \right]. \quad (4)$$

Second, let us turn to films with $d > \xi$, where the tilt modes of the vortex lattice become relevant. Close to the upper critical field we can neglect the compression and shear modes involving c_{11} and c_{66} [both proportional to $(1-b)^2$] as compared to the tilt modes with $c_{44} \propto (1-b)$. Similarly to the 2D case, where we have excluded long-wavelength contributions $K \rightarrow 0$ to the Lindemann criterion, here we exclude long-wavelength tilt modes from the integral in (2). Choosing $k_{BZ} = v\pi/a_0$ with v a numerical constant of order unity, we obtain a similar result as before in Eq. (3) but with $R^\square \rightarrow R_{\text{eff}}^\square = \rho_n v/a_0$ and f_0, f_T now replaced by

$$f_0 = \frac{1}{2} \int_0^1 dx \int_0^1 dy \ln \left[1 + \beta^2 \left(1 + \frac{\alpha^2 x}{y^2} \right)^2 \right], \quad (5)$$

$$f_T = \gamma^2 \int_0^\infty dy y (\coth y - 1) \int_0^1 dx \frac{\Theta(x - \frac{1}{2})}{x^4 + \gamma^2 y^2},$$

with the parameters $\alpha = 2/\sqrt{\pi}v$,

$$\beta = \eta\omega_{\text{max}}/c_{44}k_{BZ}^2 = 2/\pi b(1-b),$$

and

$$\gamma = t(2T_c/\epsilon_0 v a_0) [R_Q/R_{\text{eff}}^\square(1-b)b].$$

Note that close to H_{c2} we have $a_0 = \sqrt{2\pi}\xi$; the above choice for the cutoff correctly reproduces the high-temperature result for $\langle u^2 \rangle$. The $\beta \rightarrow \infty$ ($b \rightarrow 1$) limit of f_0 is $f_0 \approx \ln\beta + \alpha(2\pi/3 - \alpha/2)$, $\alpha \ll 1$. At low temperatures $f_T \approx (7\pi^2/36)\gamma^2$. The high-temperature limit $t \rightarrow 1$ is $f_T \approx (\pi/2)\gamma$, reproducing (at least parametrically) the high-temperature result²³ $\langle u^2 \rangle \approx Ta_0/\epsilon_0(1-b)$. The $T=0$ quantum melting transition takes place at a magnetic field value

$$B_m^G = H_{c2} \left\{ 1 - \frac{2}{\pi} \exp \left[\alpha \left(\frac{2\pi}{3} - \frac{\alpha}{2} \right) \right] \right. \\ \left. \times \exp \left[- \frac{\pi^3 c_L^2 R_Q}{2 R_{\text{eff}}^\square} \right] \right\}, \quad (6)$$

close to the upper critical field H_{c2} .

The melting line $B_m(T)$ and the upper critical field $H_{c2}(T)$ of amorphous Nb₃Ge have been determined resistively down to $T=38$ mK on a film with $d=300$ nm, $T_c=2.7$ K, and $\rho=200$ $\mu\Omega$ cm, using the procedure described in Ref. 21. The data for $H_{c2}(T)$ closely follow the theoretical expectations for a dirty superconductor.¹¹ For temperatures away from $T=0$ very good agreement is obtained between the data for the melting transition and the dislocation-mediated melting line $B_m^d(T)$ as given by (1) (see Fig. 3; no adjustable parameters), providing clear evidence for the topological melting scenario. At very low temperatures the data do not approach H_{c2} but extrapolate to a lower field value with $1-b_m^G \approx 4 \times 10^{-2}$. This experimental finding can be reproduced by the present theory, Eq. (6), if we choose a parameter $c_L^2/v \approx 4 \times 10^{-3}$; for a Lindemann number²⁴ $c_L=0.16$ we obtain $v \approx 6$. The corresponding melting line $B_m^G(T)$ closely follows the upper critical field line $H_{c2}(T)$ and only becomes relevant at low temperatures after its intersection with the dislocation-mediated melting line $B_m^d(T)$; see Fig. 3.

Finally, we estimate the width of the critical region. We concentrate first on the 2D case. For a simple estimate we can compare the mean-field energy density of the vortex system $\mathcal{F}_{\text{MF}} \approx [\epsilon_0 d / \xi^2] (1-b)^2$ with the shear energy density $\langle c_{66} K^2 u^2 \rangle$ due to fluctuations of the vortices. This approach correctly reproduces the ($B=0$) Ginzburg criterion close to T_c : With $\langle c_{66} K^2 u^2 \rangle \approx T/\xi^2$ we obtain the width $1-t \approx T_c/\epsilon_0(0)d$. On the other hand, we can write

$$\langle c_{66} K^2 u^2 \rangle \approx [\epsilon_0 d (1-b)^2 / a_0^2] \langle u^2 \rangle / a_0^2$$

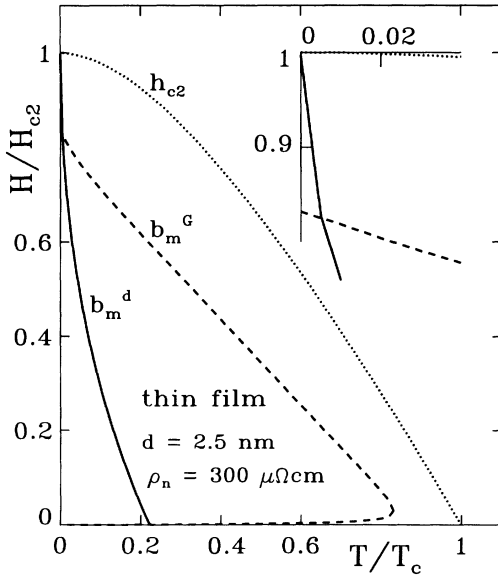


FIG. 2. H - T phase diagram for an optimized thin film. Shown are the (normalized) upper critical field line h_{c2} (dotted line), the dislocation-mediated melting line b_m^d (solid line), and the “Gaussian” melting line b_m^G (dashed line). Typical parameters for such a thin film are $T_c \approx 2$ K and $H_{c2} \approx 4$ T. The inset shows the region ($T \approx 0, H \approx H_{c2}$) on an expanded scale.

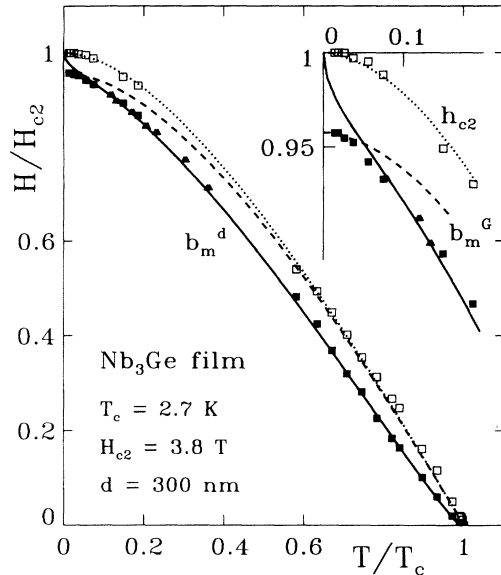


FIG 3. H - T phase diagram for a $d=300$ nm Nb_3Ge film. The upper critical field H_{c2} (open squares) and the melting line B_m (full squares, measured at constant T ; full triangles, measured at constant field) have been determined resistively. Away from zero temperature the data agree well with the dislocation-mediated melting line B_m^d (no adjustable parameters). Close to zero temperature the data cross over to the ‘‘Gaussian’’ melting line B_m^G , providing evidence for the observation of a $T=0$ quantum melting transition in a vortex system.

and extract the critical amplitude $\langle u^2 \rangle \simeq a_0^2$ by comparison with \mathcal{F}_{MF} . Since at the melting transition $\langle u^2 \rangle = c_L^2 a_0^2$ we find that due to the smallness of the Lindemann number the melting line is always outside the critical region. In 3D the mean-field energy density is $\mathcal{F}_{\text{MF}} \simeq [\varepsilon_0/\xi^2](1-b)^2$ whereas the energy density for the

tilt modes is $\langle c_{44}k_z^2 u^2 \rangle$. Again we can reproduce the ($B=0$) Ginzburg criterion close to T_c using the thermal result $\langle c_{44}k_z^2 u^2 \rangle \simeq T/\xi^3, 1-t \simeq [T_c/\varepsilon_0(0)\xi(0)]^2$. Vice versa, expressing the fluctuation contribution via $\langle u^2 \rangle$,

$$\langle c_{44}k_z^2 u^2 \rangle \simeq [\varepsilon_0(1-b)/\xi^2] \langle u^2 \rangle / a_0^2,$$

we obtain a critical amplitude $\langle u^2 \rangle \simeq (1-b)a_0^2$ and hence the applicability of our result depends on the smallness of $1-b$ as given by the criterion $1-b > c_L^2$. With $c_L=0.16$ we obtain the condition $1-b > 3 \times 10^{-2}$ and hence our calculation is at the border of the regime of its applicability.

In the above analysis we have neglected the influence of a static disorder potential leading to pinning of the vortex system. This approximation is well justified as long as the disorder is weak, e.g., in the sense that the transverse collective pinning radius²⁵ R_c is much larger than the lattice constant a_0 , a requirement usually fulfilled in the amorphous films studied here.

In conclusion, we have investigated the possibility of observing a $T=0$ quantum liquid of vortices in a type-II superconductor. We find that the most promising candidates for the observation of this effect are thin amorphous films with a high resistance placing them close to the superconductor-insulator transition. We have calculated the dislocation-mediated as well as the ‘‘Gaussian’’ melting lines and have found favorable conditions for a melting transition driven by quantum fluctuations for fields close to the upper critical field H_{c2} but still outside the critical region. The possibility that this effect has been observed in a Nb_3Ge film has been pointed out.

We wish to thank Michail Feigel'man and Maxim Kagan for helpful discussions. Financial support from the Swiss National Foundation is gratefully acknowledged.

*Permanent address: L. D. Landau Institute of Theoretical Physics, 117940 Moscow, Russia. Present address: Universidad Autonoma de San Luis Potosi, Instituto de Fisica, Alvaro Obregon 64, 78000 San Luis Potosi, S. L. P. Mexico.

†Permanent address: I. V. Kurchatov Institute of Atomic Energy, 123182 Moscow, Russia.

¹G. Blatter and B. Ivlev, Phys. Rev. Lett. **70**, 2621 (1993).

²L. Fruchter, A. Malozemoff, I. Campbell, J. Sanchez, M. Konczykowski, R. Griessen, and F. Holtzberg, Phys. Rev. B **43**, 8709 (1991).

³A.-C. Mota, G. Juri, P. Visani, A. Pollini, T. Teruzzi, K. Aupke, and B. Hilti, Physica C **185-189**, 343 (1991).

⁴R. Griessen, J. G. Lensink, and H. G. Schnack, Physica C **185-189**, 337 (1991).

⁵G. Blatter, V. B. Geshkenbein, and V. M. Vinokur, Phys. Rev. Lett. **66**, 3297 (1991).

⁶D. R. Nelson, Phys. Rev. Lett. **60**, 1973 (1988).

⁷G. Blatter and B. I. Ivlev, Phys. Rev. B **50**, 10272 (1994).

⁸M. Feigel'man, V. Geshkenbein, A. Larkin, and S. Levit, Pis'ma Zh. Eksp. Teor. Fiz. **57**, 699 (1993) [JETP Lett. **57**, 711 (1993)].

⁹N. B. Kopnin and M. M. Salomaa, Phys. Rev. B **44**, 9667 (1991).

¹⁰B. A. Huberman and S. Doniach, Phys. Rev. Lett. **43**, 950 (1979).

¹¹E. Helfand and N. R. Werthamer, Phys. Rev. **147**, 288 (1966).

¹²A. A. Abrikosov, L. P. Gor'kov, and I. E. Dzyaloshinski, *Methods of Quantum Field Theory in Statistical Physics* (Dover, New York, 1975).

¹³D. S. Fisher, Phys. Rev. B **22**, 1190 (1980).

¹⁴Y. Kato and N. Nagaosa, Phys. Rev. B **47**, 2932 (1993).

¹⁵S. Ryu, S. Doniach, G. Deutscher, and A. Kapitulnik, Phys. Rev. Lett. **68**, 710 (1992).

¹⁶D. Ceperley, Phys. Rev. B **18**, 3126 (1978). Note that quantum and thermal fluctuations enter the melting criterion differently and thus c_L may change with temperature.

¹⁷L. D. Landau and E. M. Lifshitz, *Statistical Physics* (Pergamon, London, 1958).

¹⁸E. H. Brandt, J. Low Temp. Phys. **26**, 709 (1977).

¹⁹V. L. Berezinskii, Zh. Eksp. Teor. Fiz. **59**, 907 (1970) [Sov. Phys. JETP **32**, 493 (1971)].

²⁰J. M. Graybeal, Physica B + C **135B**, 113 (1985).

²¹P. Berghuis and P. H. Kes, Phys. Rev. B **47**, 262 (1993).

²²D. B. Haviland, Y. Liu, and A. M. Goldman, Phys. Rev. Lett. **62**, 2180 (1989).

²³A. Houghton, R. A. Pelcovits, and A. Sudbø, Phys. Rev. B **40**, 6763 (1989).

²⁴The melting line in a 2.4- μm -thick film (Ref. 21) is well described by the 3D melting criterion (Ref. 23) with $c_L=0.16 \pm 0.01$.